

Development a Numerical Model Applicable to Inorganic and Organic Solar Cells Based on Silicon in the Presence of Excitons

¹Modou FAYE, ²Cheikh MBOW, ¹Bassirou BA

¹Laboratory of Semiconductors and Solar Energy, Physics Departement, Faculty of Science and Technology University Cheikh Anta DIOP-Dakar-SENEGAL, fayendiouma@yahoo.fr.

²Laboratory Hydraulics and Transfers, Physics Departement, Faculty of Science and Technology University Cheikh Anta DIOP-Dakar-SENEGAL.

Abstract – The solar cell under monochromatic illumination by the front face and subjected to a heat insulation by the back face in permanent regime is studied. The continuity equations for electrons and excitons coupled and the heat, which govern the generation-recombination and diffusion mechanisms have been solved by a numerical approach based on the finite volumes method.

These mechanisms are analyzed through the profile of the density total photocurrent, calculated for different values of the excitation wavelength and the volume and surface conversion coefficients which respectively depend on exciton dissociation field and the average temperature.

The effects of the heating factor and the number of Fourier on the electron and exciton particle current were analyzed.

In the end, a comparison between the electron and exciton particle current calculated as functions of two forms of volume coupling coefficient has also been proposed. This study allowed us to achieve our objective, namely the development of a numerical model applicable to inorganic and organic solar cells.

Keywords – Electric field, excitons, Average temperature, heating factor, number of Fourier, photocurrent.

1 INTRODUCTION

The production of energy from solar cells is a major challenge now and in the coming years. Also to prevent pollution, to enable future generations to access to natural resources and improve the conversion efficiency finally deal with any imbalances between supply and strong demand, it is important towards numerical models. Some authors like Mr. Burgelman and B. Minnaer [2] developed a numerical model applicable to organic solar cells in the presence of excitons.

The objective of our study is to develop a numerical model applicable to inorganic and organic solar cells in the presence of excitons for different values of volume coupling and surface conversion coefficients. We performed by considering a solar cell subjected monochromatic illumination from the front side and a thermal insulation from the back side by taking into

account inclusion of the space charge zone and the non-uniformity of the dissociation and recombination of excitons in this zone. This model is governed systems of equations coupled non-linear partial derivatives which we do not know the analytical solutions in general. That is why our choices have been focused on the mathematical and numerical models. The equations of continuous domain are integrated by the control volume method and the coefficients of algebraic systems are approached by the scheme of Patankar. Finally, we solve them by using an iterative relaxation line by line type Gauss Siedel.

2 POSITION OF THE PROBLEM AND MATHEMATICAL FORMULATION

2.1 Physical position of the problem and Assumptions

We will consider a semiconductor of length L (Figure 1), a one-dimensional character, and the non-uniform doped regions. They are conductive. The electric field in the space charge zone is not negligible. We admit that this electric field in the space charge zone is a linear function of the abscissa z that can be expressed in the form

$$E(z) = \frac{E_m}{w}(w-z) \text{ and } b(z) = b[E(z)] \text{ in } (0 \leq z \leq w)$$

We have also taken into account the absorption due to the charge carriers such as $f_e + f_x = 1$ [2]. With f_e is the fraction of electrons and f_x is that the excitons. We consider for an inorganic solar cell ($f_e = 1$ and $f_x = 0$) and an organic solar cell ($f_e = 0$ and $f_x = 1$).

The majority carriers are not affected and regarding the minority carriers, their distributions are governed by the continuity equations.

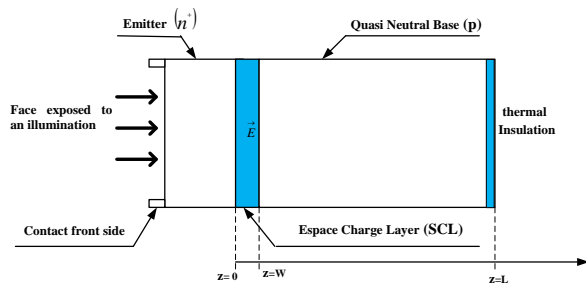


Figure 1: n⁺p solar cell silicon under monochromatic illumination

In addition we assume that faces $z=0$ and $z=L$ are the site of recombination events in volume and surface. The electron diffusion coefficients and excitons are functions of some variables, particularly the temperature of the material. They are given by the Einstein relation [11].

2.2 Mathematical formulation

Considering the modeling assumptions above and the following reference physical quantities C_r (concentration for carriers), $\Delta T_r = \frac{q_m \times L}{\lambda}$ (for the temperature difference), L and W (for the spatial variables z), G_r (generation rate of carriers and that of excitons), the non-dimensional equations for the coupled system and the heat become:

$$F_{e0} \frac{\partial}{\partial z^*} \left\{ D_r^* \frac{\partial n_e^*}{\partial z^*} \right\} + A \frac{\partial}{\partial z^*} \left\{ n_e^* (w^* - z^*) \right\} = \frac{n_e^* n_h^* - n_{in}^{*2}}{n_e^* + n_h^* + 2n_{in}^*} + B_e (n_e^* n_h^* - n_e^* n_i^*) - C_e f_e G^* \quad (1a)$$

$$F_{x0} \frac{\partial}{\partial z^*} \left\{ R_\mu D_r^* \frac{\partial n_x^*}{\partial z^*} \right\} = (n_x^* - n_{x0}^*) - B_x (n_e^* n_h^* - n_x^* n_i^*) - C_x (1 - f_e) G^* \quad (1b)$$

$$\frac{\partial T^*}{\partial z^*} = \frac{\partial^2 T^*}{\partial z^{*2}} \quad (2)$$

Along with

$$z^* = \frac{z}{L}, \quad z^* = \frac{W}{L}, \quad n_e^* = \frac{n_e}{C_r}, \quad n_h^* = \frac{n_h}{C_r}, \quad n_x^* = \frac{n_x}{C_r},$$

$$n_{in}^* = \frac{n_{in}}{C_r},$$

$$G^* = \frac{G_{eh}}{G_r}, \quad G^* = \frac{G_x}{G_r}, \quad t^* = \frac{a}{L^2} t, \quad T^* = \frac{T - T_a}{\Delta T_r}$$

The amount D^0 is the electron diffusion coefficient calculated from the ambient temperature T_a considered constant. The "diffusion coefficient" dimensionless D_T^* expressed as:

$$D_T^* = 1 + \frac{\Delta T_r^*}{T_a} T^* \quad (3)$$

is therefore a function of the dimensionless temperature

T^* . The amount $\frac{\Delta T_r^*}{T_a}$ is called heat factor. To

complete the system of equations (1) and (2) in the interval $[0,1]$, we associate the initial conditions and the conditions to which their limits dimensionless expressions are shown in Table 1 below

Table 1:

Initial and boundary conditions associated of the dimensionless electrons, excitons and the temperature

For the electrons	For the excitons
$z^* = 0 \Rightarrow n_e^*(0) = N_D^*$	$z^* = 0 \Rightarrow A_{0x} \frac{\partial}{\partial z^*} \{ R_\mu D_r^* n_x^* \}_{z=0} = [n_x^*(0) - n_{x0}^*] - B_{0x} [n_x^*(0) - n_{x1}^*]$
$z^* = 1 \Rightarrow A_{Lx} \frac{\partial}{\partial z^*} \{ D_r^* n_e^* \}_{z=1} = -[n_e^*(1) - n_{e0}^*] + B_{Lx} [n_x^*(1) - n_{x1}^*]$	$z^* = 1 \Rightarrow A_{Lx} \frac{\partial}{\partial z^*} \{ R_\mu D_r^* n_x^* \}_{z=1} = -[n_x^*(1) - n_{x0}^*] - B_{Lx} [n_x^*(1) - n_{x1}^*]$
Conditions on the temperature $t^* = 0 \Rightarrow T^*(z^*, 0) = 0$ $z^* = 0 \Rightarrow \frac{\partial T^*}{\partial z^*} = -g(t^*)$ $z^* = 1 \Rightarrow \frac{\partial T^*}{\partial z^*} = 0$	

3 NOMENCLATURE

Latin Letters:

a	thermal diffusivity [$\text{cm}^2 \text{s}^{-1}$]
C	Density equivalent status [m^{-3} or cm^{-3}]
D	diffusion coefficient [$\text{cm}^2 \text{s}^{-1}$]
E	Electric field [Vm^{-1}]
Fact_ch	Factor heated
Fo	Relationship between time diffusion and convection
G	generation rate [$\text{N cm}^{-3} \text{s}^{-1}$]
K	Boltzmann constant [JK^{-1}]
L	The diffusion length [cm]
n	Concentration of carriers, [m^{-3} or cm^{-3}]
q	Electric charge [C]
R	Rate of exciton recombination of electrons [$\text{cm}^{-3} \text{s}^{-1}$]
S	Speed of recombination [cms^{-1}]
t	time [s]
T	Temperature dimensional [K]
U	recombination rate [$\text{cm}^{-3} \text{s}^{-1}$]
W	width of the depletion zone [cm]

Greek symbols:

α	absorption coefficient [μm^{-1}]
λ	wavelength of the light source [μm]
μ	mobility of electrons and excitons [$\text{cm}^2 \text{v}^{-1} \text{s}^{-1}$]
ρ	Average density of the semiconductor, [kg m^{-3}]
τ	lifetime of electrons and excitons [s]

Indices Exhibitor:

A	acceptor
D	donor
e	on the electron
x	relative to the exciton
h	relative to the hole
in	intrinsic
m	average
o	at equilibrium
i	th component
(*)	Related to the dimensionless variables
(°)	Relative to a constant

Dimensionless numbers characteristics:

$$F_0 = \frac{\tau \times D^0}{L^2} \quad \text{Relationship between the broadcasting time and life}$$

$$Fact_ch = \frac{\Delta T_r}{T_a} \quad \text{Relationship between heat flux imposed and conduction}$$

$$R_\mu = \frac{\mu_x}{\mu_e} \quad \text{relationship between the mobility of excitons and electrons}$$

4 NUMERICAL PROCEDURE

The mathematical formulation of our physical problem involves three differential partial differential equations that must be solved to find a solution to the problem in question. In this case, the only way that we can provide an appropriate solution consists of the numerical

approach. Before the digital process, the mathematical formulation is to be transformed by means of a discretization process to achieve an easy. In our present study, we chose the finite volume method.

It is to discretize the computational domain into a number of finite volumes called volume controls (V_c) in which the transport equations are integrated [5].

First we will approach the continuous segment [0, 1] in a series of i_m points (nodes) of x-rated z_i . As different parts of our area (the space charge zone and the base) are not the same size and are the site of physical phenomena of very different natures should be used a variable mesh. The distributions of electrons and excitons are very sensitive to surface phenomena and a neighborhood in fine mesh adopted. And the different zones are approximated by:

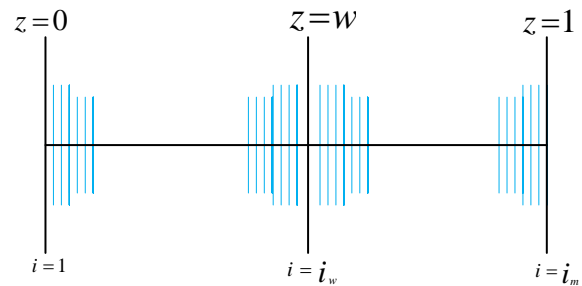


Figure 2: Schematics of our mesh

In the space charge zone

$$z_i = w \times \tan \left[\frac{\pi}{4} \times \frac{(i-1)}{i_w - 1} \right] \quad (4)$$

In the base

$$z_i = w + (1-w) \times \left\{ \tan \left[\frac{\pi}{4} \times \frac{(i-i_w)}{i_m - i_w} \right] \right\} \quad (5)$$

Along with i_w the index that identifies the position of the load zone interface space / base.

The discretization of the equations and the boundary conditions, Systems solving method of nonlinear equations obtained and the different steps of the algorithm are already developed, specified and explained in [5].

5 RESULTS AND DISCUSSION

To validate our code, we compared our results with those of Mr. Burgelman and B. Minnaer [2].

The results from the mathematical and numerical modeling of various phenomena are summarized by considering the representation below.

We essentially present the influences of surface conversion and volume coupling coefficients, of the heating factor and the number of Fourier total photocurrent density of electrons and excitons in the junction.

The tests we conducted showed that the time step, the index that tracks the position of the load area space

interface / base, the number of nodes, the permitted relative error and the relaxation parameter $\delta t^* = 10^{-3}$; $i_w = 81$; $i_m = 201$; $\varepsilon = 10^{-3}$ and $w = 0.15$ are a good compromise between an acceptable calculation volume and a reasonable calculation time. We used the volume coupling coefficient in two forms: we have expressed in terms of exciton dissociation field and the mean temperature

$$bv\{E(z)\} = bv_low \times \exp\left[\left(1 - \frac{z}{w}\right) \times \ln\left(\frac{bv_max}{bv_low}\right)\right] \text{ and}$$

only according to the average temperature $bv(T_{moy}) = (10^{-2} \times T_{moy}^{-2} + 2.5 \times 10^{-6} \times T_{moy}^{-0.5} + 1.5 \times 10^{-7})$ [2] and [5].

Along with $bv_low = 10^{-16} \text{ cm}^3 \text{ s}^{-1}$, $10^{-16} \text{ cm}^3 \text{ s}^{-1} \leq bv_max \leq 10^{-7} \text{ cm}^3 \text{ s}^{-1}$ and T_{moy} the average temperature. We have considered these expressions volumetric coupling coefficient only in the space charge zone. In the database, for each of these forms of the coupling coefficient we took $bv = bv_low = 10^{-16} \text{ cm}^3 \text{ s}^{-1}$.

Assuming a negligible electric field polarization in the database, the photocurrent densities of electrons and excitons are given by the gradient of the charge carriers at the junction.

The density of photocurrent of electrons at the interface is defined by:

$$J_e = q \times j_e \quad (6)$$

Along With

$$j_e = J_r \times J_e^* \quad ; \quad J_r = \frac{D_o \times C_r}{L} \quad \text{et} \quad J_e^* = D_T \left. \frac{\partial n_e^*}{\partial z^*} \right|_{z=1}$$

the junction we are in the presence of a potential gradient and a concentration gradient.

The density of photocurrent of excitons at the junction is defined in the presence of a concentration gradient:

$$J_x = q \times R_\mu \times J_r \times J_x^* \quad (7)$$

$$\text{Along With } J_x^* = D_T \left. \frac{\partial n_x^*}{\partial z^*} \right|_{z=1}$$

The density total of photocurrent of the solar cell is equal to the sum of those electrons and excitons to a monochromatic illumination through the front:

$$J = J_e + J_x \quad (8)$$

5.1 Total photocurrent density at the junction depending on the wavelength: Influence of absorption due to electron-hole pairs

To study the influence of the wavelength on the density total of photocurrent, the thickness of the emitter is attached to 30 nm . This type of transmitter is doped 10^{-19} cm^{-3} . It has a very important phenomenon of diffusion. The different wavelengths of the monochromatic light of the solar cell are selected from

the range: $0.70 \mu\text{m} \leq \lambda \leq 1.05 \mu\text{m}$, corresponding to the main absorption depths allowing exploration of the entire volume of the solar cell.

The curves in Figure 3 show that, if the absorption is divided into two, one half absorbed by the electrons and the other half by the excitons, the photocurrent increases. This increase is more important when we are in the case of inorganic semiconductors, ie for absorption predominated by the electrons.

For wavelengths greater than approximately $1.05 \mu\text{m}$, the density of photocurrent decreases. The explanation for this decrease is that the wavelengths correspond to low intensities of light and therefore the charge carriers decrease photogenerated.

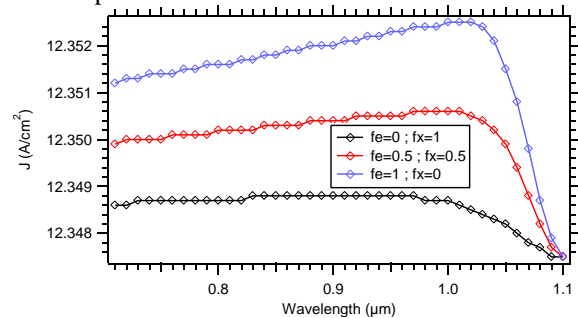


Figure 3: Influence of absorption of the variation of the density total of photocurrent of the charge carriers for a silicon solar cell

$N_A = 10^{16} \text{ cm}^{-3}$; $N_D = 10^{19} \text{ cm}^{-3}$; $n_i = 1.45 \cdot 10^{10} \text{ cm}^{-3}$;
 $n_mott = 1.031 \cdot 10^{18} \text{ cm}^{-3}$; $Se = Sx = 10 \text{ cm s}^{-1}$; $Fo = 10$;
 $Fact_ch = 2 \cdot 10^{-2}$; $bv_low = 10^{-16} \text{ cm}^3 \text{ s}^{-1}$; $bv_max = 10^{-7} \text{ cm}^3 \text{ s}^{-1}$;
 $bs_max = 10^{+1} \text{ cm s}^{-1}$; $L_e \neq L_x = f$ (average temperature)

Our goal is to develop a numerical model applicable to inorganic and organic semiconductors.

Now we will see the influence of absorption on the total photocurrent density as a function of volume coupling and surface conversion normalized coefficients.

5.2 Density total of photocurrent at the junction as a function of the normalized coefficient

In this section we study the evolution of the density total of photocurrent as a function of the volume or surface conversion coefficient. It will allow us to draw a conclusion on making our electronic device.

5.2.1 Influence of absorption due to electron-hole pairs

The absorption due to electron-hole pairs has a negligible effect on the density total of photocurrent of the charge carriers. This total photocurrent density calculated from the volume coupling coefficient is higher than that obtained with the planar coefficient. The density total of photocurrent increases with weak coefficients. From some of the values of the coefficient, it reaches a limit value. Once this value is reached the density total of photocurrent remains constant whatever the values of the normalized coefficient. We see later in our simulation, this asymptote showing the operation of the current generator solar cell under monochromatic illumination from the front, is observed for bv or bs (normalized).

Indeed, all holders across the junction to participate in the photocurrent.

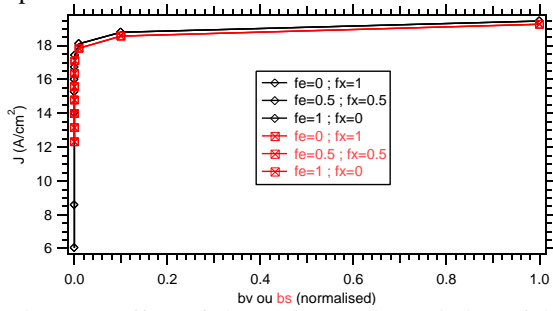


Figure 4: Effect of absorption on the variation of the density of photocurrent of the charge carriers for a silicon solar cell
 $N_A=10^{16} \text{ cm}^{-3}$; $N_D=10^{19} \text{ cm}^{-3}$; $n_i=1.45 \cdot 10^{10} \text{ cm}^{-3}$;
 $n_{\text{mott}}=1.031 \cdot 10^{18} \text{ cm}^{-3}$; $Se=S_x=10 \text{ cm s}^{-1}$; $Fo=10$;
 $\text{Fact}_{\text{ch}}=2 \cdot 10^{-2}$; $\alpha(\lambda)=0$; $bv_{\text{low}}=10^{-16} \text{ cm}^3 \text{ s}^{-1}$;
 $bv_{\text{max}}=10^{-7} \text{ cm}^3 \text{ s}^{-1}$; $bs_{\text{max}}=10^{+1} \text{ cm s}^{-1}$; $L_e \neq L_x=f$
 (average temperature)

The results of the fig 4 confirm that we can design our model based on the volume or surface conversion coefficient. It allows us to achieve high density of photocurrent, see a maximum quantum efficiency.

5.2.2 Volume coupling coefficient Influence

The results in Figure 5 show that low- and middle-couplings excitons are completely dissociated, while the strong coupling we have the opposite effect. In addition, as can be seen in Figure 5, there is a volume coupling coefficient threshold, $bv_{\text{max}} = 10^{-8} \text{ cm}^3 \text{ s}^{-1}$, from which the total photocurrent density of charge carriers increases. It is from this factor that we have a strong field exciton dissociation. These results indicate that for low values of the volume of coupling coefficient recombination predominates the heat generation. While for large values of the volume coupling coefficient is the thermo generation predominates over recombination.

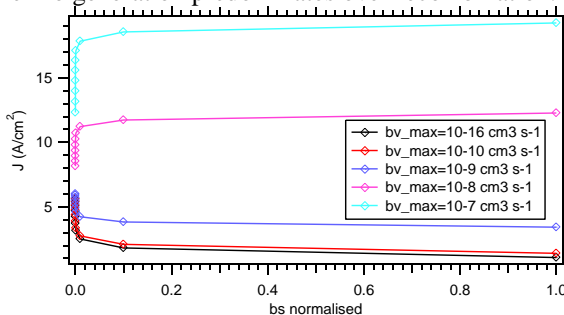


Figure 5: Influence of the volume coupling coefficient on the change in the charge carriers of photocurrent for a silicon solar cell
 $N_A=10^{16} \text{ cm}^{-3}$; $N_D=10^{19} \text{ cm}^{-3}$; $n_i=1.45 \cdot 10^{10} \text{ cm}^{-3}$;
 $n_{\text{mott}}=1.031 \cdot 10^{18} \text{ cm}^{-3}$; $Se=S_x=10 \text{ cm s}^{-1}$; $f_x=0$; $f_c=1$;
 $Fo=10$; $\text{Fact}_{\text{ch}}=2 \cdot 10^{-2}$; $bv_{\text{low}}=10^{-16} \text{ cm}^3 \text{ s}^{-1}$; $L_e \neq L_x=f$
 (average temperature)

5.2.3 Influence of surface conversion coefficient

In Figure 6, we calculated the density total of photocurrent for four values of surface conversion

coefficient. These results show that the increase in total photocurrent for a given value of the conversion coefficient starts from $bs_{\text{max}} = 10^{+3} \text{ cm s}^{-1}$. To values less than this value the surface conversion coefficient to a non-significant effect on the photocurrent. The boundary conditions show the surface conversion coefficient and the recombination velocity are inversely proportional. Indeed to minimize recombination losses must realize this model with large values of the surface conversion coefficient.

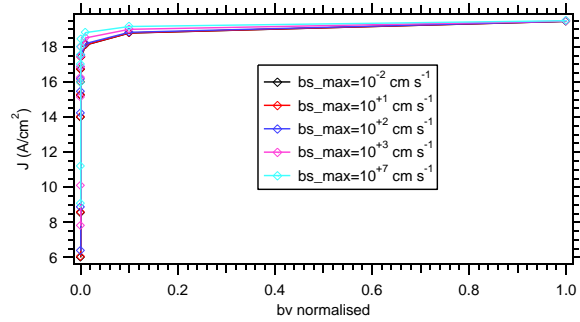


Figure 6: Influence of surface conversion coefficient on the change in the charge carriers of photocurrent for a silicon solar cell

$N_A=10^{16} \text{ cm}^{-3}$; $N_D=10^{19} \text{ cm}^{-3}$; $n_i=1.45 \cdot 10^{10} \text{ cm}^{-3}$;
 $n_{\text{mott}}=1.031 \cdot 10^{18} \text{ cm}^{-3}$; $Se=S_x=10 \text{ cm s}^{-1}$; $f_x=0$; $f_c=1$;
 $Fo=10$; $\text{Fact}_{\text{ch}}=2 \cdot 10^{-2}$; $bv_{\text{low}}=10^{-16} \text{ cm}^3 \text{ s}^{-1}$; $L_e \neq L_x=f$
 (average temperature)

5.2.4 Influence of the heating factor

The effect of the volume of coupling coefficient of the variation of the density total of photocurrent requires no threshold value of the surface conversion coefficient. The increase of the density of photocurrent is much sharper with those of the large values of the heating factor. This setting increases the number of carriers stored at interfaces and excited likely to participate in the photocurrent. The effects of the heating factor and the number of Fourier average temperature are synonymous. Their variation leads that of the average temperature, which will cause the exciton dissociation field.

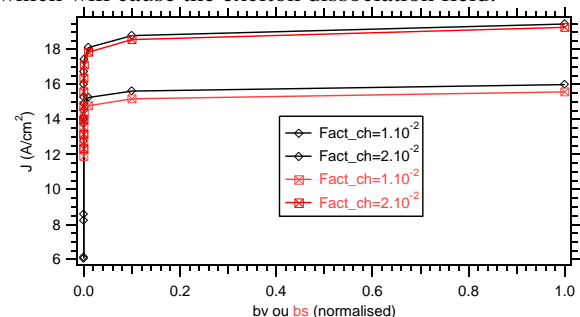


Figure 6: Influence of surface conversion coefficient on the change in the charge carriers of photocurrent for a silicon solar cell
 $N_A=10^{16} \text{ cm}^{-3}$; $N_D=10^{19} \text{ cm}^{-3}$; $n_i=1.45 \cdot 10^{10} \text{ cm}^{-3}$;
 $n_{\text{mott}}=1.031 \cdot 10^{18} \text{ cm}^{-3}$; $Se=S_x=10 \text{ cm s}^{-1}$; $f_x=0$; $f_c=1$;
 $Fo=10$; $bv_{\text{low}}=10^{-16} \text{ cm}^3 \text{ s}^{-1}$; $bv_{\text{max}}=10^{-7} \text{ cm}^3 \text{ s}^{-1}$;
 $bs_{\text{max}}=10^{+1} \text{ cm s}^{-1}$; $L_e \neq L_x=f$ (average temperature)

5.2.5 Influence of the number of fourier

Figure 8 represents the values of the density total of photocurrent for two values of the number of fourier. It shows that the density total of photocurrent rapidly increases with larger values of the number of fourier. In explanation we'll say the increase fourier leads that of the average temperature. While the increase of the average temperature also causes the electric field exciton dissociation. Therefore the increase in charge carrier photocurrent density is due to a simultaneous increase in the average temperature and the electric field.

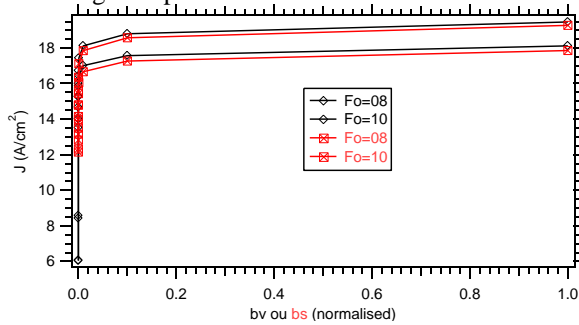


Figure 8: Influence of the number of fourier on the variation of the charge carriers of the photocurrent for a silicon solar cell

$N_A=10^{16} \text{ cm}^{-3}$; $N_D=10^{19} \text{ cm}^{-3}$; $n_i=1.45 \cdot 10^{10} \text{ cm}^{-3}$;
 $n_{\text{mott}}=1.0310^{18} \text{ cm}^{-3}$; $Se=S_x=10 \text{ cm s}^{-1}$; $f_x=0$; $f_e=1$;
 $Fact_{\text{ch}}=2 \cdot 10^{-2}$; $bv_{\text{low}}=10^{-16} \text{ cm}^3 \text{ s}^{-1}$; $bv_{\text{max}}=10^{-7} \text{ cm}^3 \text{ s}^{-1}$;
 $bs_{\text{max}}=10^{+1} \text{ cm s}^{-1}$; $L_e \neq L_x=f$ (average temperature)

5.3 Validation of the model

The evolution of the curves in Figure 9 show that the values of the density total of photocurrent denoted with a solid coupling coefficient $bv(T_{\text{moy}})$ are higher than those obtained with the coefficient $bv\{E(z)\}$. We recall that the influence of each of these coefficients is limited at the space charge zone at the base because we have set $bv_{\text{low}}=10^{-16} \text{ cm}^3 \text{ s}^{-1}$. In this area the coefficient $bv(T_{\text{moy}})=3 \cdot 10^3 \text{ cm}^3 \text{ s}^{-1}$, whereas $bv\{E(z)\}$ varies $10^{-16} \text{ cm}^3 \text{ s}^{-1} \leq bv\{E(z)\} \leq 10^{-7} \text{ cm}^3 \text{ s}^{-1}$. In the strong coupling $bv(T_{\text{moy}})$, the density of the created image bearers participating in the photocurrent is higher than that obtained in the case of weak and means conversion coefficients. Therefore we can design a model applicable to inorganic and organic semiconductors with a coupling coefficient that depends simultaneously the dissociation of excitons and the average temperature field, but this model is larger with a coupling coefficient which is function of the average temperature.

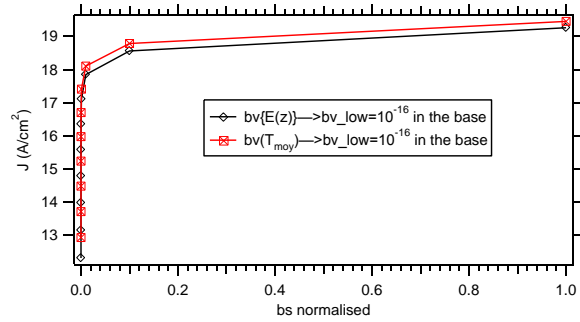


Figure 9: Influence of surface conversion coefficient on the variation of the load carriers of the photocurrent for a silicon solar cell

$N_A=10^{16} \text{ cm}^{-3}$; $N_D=10^{19} \text{ cm}^{-3}$; $n_i=1.45 \cdot 10^{10} \text{ cm}^{-3}$;
 $n_{\text{mott}}=1.0310^{18} \text{ cm}^{-3}$; $Se=S_x=10 \text{ cm s}^{-1}$; $f_x=0$; $f_e=1$;
 $Fo=10$; $Fact_{\text{ch}}=2 \cdot 10^{-2}$; $bv_{\text{low}}=10^{-16} \text{ cm}^3 \text{ s}^{-1}$;
 $bv_{\text{max}}=10^{-7} \text{ cm}^3 \text{ s}^{-1}$; $L_e \neq L_x=f$ (average temperature)

6 CONCLUSION

The numerical study of the influence of the wavelength and of the volume coupling or surface conversion coefficient on the density total of photocurrent of electrons and excitons in a silicon solar cell was presented. The geometric configuration of the physical model is a solar cell junction n^+p by the model of the extension of the space charge zone. It is subjected to monochromatic illumination and thermal insulation from the rear side. The numerical study was undertaken to identify the appropriate parameters for designing a digital model applicable to inorganic and organic semiconductors.

After introducing the basic equations governing mechanisms of generation-recombination and diffusion, we were interested in the simulation. She used the method of Patankar control volume and an implicit scheme little cost in time and Volume discretization adimensionnalized equations. Algebraic equations were solved by the double sweep method.

The computer code that we developed was validated by the results of work in the literature.

It is apparent from our study that the influence of the wavelength on the density total of photocurrent is greater in the case of an inorganic semiconductor. The influence of standardized coefficients on density total of photocurrent has enabled us to develop a numerical model applicable to inorganic and organic semiconductors. Certain physical parameters such as the heating factor and the number of fourier have positive effects on the density total of photocurrent of charge carriers.

It also appears from our results an interesting comparative study between total photocurrent densities obtained with two expressions of volume coupling coefficient. It is interesting because it has allowed us to improve the density total of photocurrent therefore to provide application domain in engineering.

APPENDIX

$$A = \frac{\mu_e \tau_e E_m}{w}; A_{eL} = \frac{D^0}{LS_e}; A_{xL} = \frac{D^0}{LS_x}; A_{0x} = \frac{D^0}{LS_{0x}}$$

$$B_{eL} = \frac{b_s}{S_e}; B_{xL} = \frac{b_s}{S_x}; B_{0x} = \frac{b_s}{S_{0x}}; B_e = \tau_e b C_r; B_x = \tau_x b C_r$$

$$C_e = \frac{\tau_e G_r}{C_r}; C_x = \frac{\tau_x G_r}{C_r}$$

$$\alpha(\lambda) = 0.526367 - 1.14425 / \lambda + 0.585368 / \lambda^2 + 0.039958 / \lambda^3$$

REFERENCES

- [1] D. E. Kane, R. M. Swanson: The effects of excitons on apparent band gap narrowing and transport in semiconductors, *J. Appl. Phys.* 73, 1193-1197 (1993).
- [2] M. Burgelman, B. Minnaert ; Including excitons in semiconductor solar cell modeling. *Thin Solid Films* 511-512, 214-218 (2006).
- [3] S. Zh. Karazhanov ; Temperature and doping level dependence solar cell performance Including excitons. *Solar Energy Materials & Solar Cells* 63 (2000) 149-163.
- [4] R. Corkish, D. S. P. Chan, and M. A. Green ; Excitons in silicon diodes and solar cells: A three-particle theory. Institute of Physics. [(S0021-8979(1996) 0070-9)].
- [5] M. Faye, M. MBow, M. Ba: Numerical Modeling of the Effects of Excitons in a Solar Cell Junction n⁺p of the Model by Extending the Space Charge Layer, *International Review of Physics (I.RE.PHY)*, Vol. 8, N. 4 ISSN 1971-680X (August 2014)
- [6] Y.Zhang, A.Mascarenhas, S. Deb: Effets of excitons in solar cells *J. Appl. Phys.* 84 3966-3971 3966 (1998).
- [7] Chunjun Liang^{a,*}, Yongsheng Wang^a, Dan Li^b, Xingchen Ji^b, Fujun Zhang^a, Zhiquan He^a ; Modelind and simulation of bulk heterojunction polymer solar cells. *Solar Energy Materials & Solar Cells* 127 (2014) 67-86.
- [8] V. A. Trukhanov, V.V. Bruevich, D.Yu. Paraschuk ; Effect of doping on performance of organic solar cells. International Laser Center and Faculty of Physics, M.V. Lomonosov Moscow State University, Moscow 119991, Russia (Dated: December 1, 2011)
- [9] Ji-Ting Shieh,¹ Chiou-Hua Liu,² Hsin-Fei Meng,^{3,a} Shin-Rong Tseng,³ Yu-Chiang Chao,³ and Sheng-Fu Horng² ; The effect of carrier mobility in organic solar cells. *JOURNAL OF APPLIED PHYSICS* **107**, 084503 2010.
- [10] S.V.Patankar: "Numerical Heat Transfer and Fluid Flow", Hemisphere Publishing Corporation, McGraw-Hill Book Company, 1981.
- [11] R. B. BIRD, W. E. STEWART, E N. LIGHTFOOT: *Transport Phenomena*, John Wiley and Sons, Inc, New York 2001.

- [12] D. W. PEACEMAN, H. A. RACHFORD, The Numerical Solution of Parabolic and Elliptic Difference Equations, *J. Soc. Ind., Appli. Math*, 3,